Dominant $(g_{9/2})^2$ neutron configuration in the 4_1^+ state of ^{68}Zn based on new g factor measurements

J. Leske,[1] K.-H. Speidel,[1] S. Schielke,[1] J. Gerber,[2] P. Maier-Komor,[3] T. Engeland,[4] and M. Hjorth-Jensen[4,*]
[1]*Helmholtz-Institut für Strahlen und Kernphysik, Universität Bonn, Nussallee 14-16, D-53115 Bonn, Germany*
[2]*Institut de Recherches Subatomiques, F-67037 Strasbourg, France*
[3]*Physik-Department, Technische Universität München, James-Franck-Strasse, D-85748 Garching, Germany*
[4]*Department of Physics and Center of Mathematics for Applications, University of Oslo, N-0316 Oslo, Norway*
(Received 5 July 2005; published 12 October 2005)

The g factor of the 4_1^+ state in ^{68}Zn was remeasured with improved energy resolution of the detectors used. The value obtained is consistent with the previous result of a negative g factor, thus confirming the dominant $0g_{9/2}$ neutron nature of the 4_1^+ state. In addition, the accuracy of the g factors of the 2_1^+, 2_2^+, and 3_1^- states has been improved and their lifetimes were well reproduced. New large-scale shell-model calculations based on a ^{56}Ni core and a $0f_{5/2}1p0g_{9/2}$ model space yield a theoretical value, $g(4_1^+) = +0.008$. Although the calculated value is small, it cannot fully explain the experimental value, $g(4_1^+) = -0.37(17)$. The magnitude of the deduced $B(E2)$ of the 4_1^+ and 2_1^+ transitions is, however, rather well described. These results demonstrate again the importance of g factor measurements for nuclear structure determinations because of their specific sensitivity to detailed proton and neutron components in the nuclear wave functions.

DOI: 10.1103/PhysRevC.72.044301 PACS number(s): 21.10.Ky, 25.70.De, 27.50.+e

I. INTRODUCTION

Measurements of nuclear magnetic dipole and electric quadrupole moments provide valuable insights into the nuclear structure based on the intriguing interplay of single-particle and collective degrees of freedom. In particular, nuclei in the *sd*- and *fp*-shell-model space have recently received considerable attention through many new experiments inspired by the unique possibility of comparing extensive data with results from large-scale shell-model calculations. This progress is also related to the observation that general features of the nuclear medium can be studied in lighter nuclei as well. For instance, superdeformation, which had been exclusively investigated for a long time on nuclei in the rare-earth mass region and beyond [1], has recently been observed in ^{36}Ar [2], ^{40}Ca [3], ^{60}Zn [4], and ^{62}Zn [5]. The obvious advantage in all these cases is the possibility of directly comparing data with structure calculations based on highly developed nuclear shell-model codes, thus providing new features of this phenomenon and collectivity in general on a microscopic nonphenomenological level.

In the same context measurements of g factors and $B(E2)$ values have been carried out for even-A Zn isotopes, with $A =$ 62–70 [6]. Two sets of large-scale shell-model calculations were applied, based on either a ^{40}Ca core and an *fp*-shell-model space or a ^{56}Ni core and an *fpg*-shell configuration space with the inclusion of the $0g_{9/2}$ orbital; the latter was considered to be particularly important for the heavier Zn isotopes. In these measurements Coulomb excitation of 160-MeV Zn projectiles was achieved in collisions with a carbon target employing inverse kinematics. At this beam energy essentially the first 2^+ states were strongly excited whereas higher-lying states were only weakly populated.

This deficiency was overcome in a succeeding experiment aiming at higher excitation energies of both ^{64}Zn and ^{68}Zn by an increase in the projectile energies to 180 MeV close to the Coulomb barrier [7]. In these new measurements the g factors and the $B(E2)$ values of the now-accessible 4_1^+ states were determined for the first time. Whereas the $g(4_1^+)$ value of ^{64}Zn was found to be consistent with predictions of both the collective and the spherical shell models, the value for ^{68}Zn of $g(4_1^+) = -0.4(2)$ turned out to be in severe conflict with both model predictions. The negative sign of the g factor was a clear indication for a dominant $0g_{9/2}$ neutron component in the wave function, whereby the Schmidt value is $g_{\mathrm{Schmidt}} = -0.425$, which, however, was not verified by the calculations. On the other hand, the newly determined $B(E2)$ values were very well explained by these shell-model calculations based on a ^{56}Ni core plus $0g_{9/2}$ neutrons. Evidently, in this case the explicit inclusion of the $0g_{9/2}$ orbital seems to be crucial for ^{68}Zn, as the alternative calculations, assuming an inert ^{40}Ca core but excluding the $0g_{9/2}$ orbital, underestimate the experimental $E2$ strength.

To set the g factor result of the ^{68}Zn(4_1^+) state on more solid ground, new measurements have been performed. As emphasized in Ref. [7], such an effort is required as in the previous measurements the energy resolution of the NaI(Tl) scintillators used for γ detection did not allow fully separating the relevant $(4_1^+ \rightarrow 2_1^+)$ γ line from a neighboring $(2_3^+ \rightarrow 2_1^+)$ 1261-keV line. As the latter was also strongly Doppler shifted because of the short nuclear lifetime, the separation of the two γ lines was particularly crucial for the detector pair placed in the forward hemisphere. On the other hand, estimates of an eventual admixture of the 2_3^+ state to the measured precession of the 4_1^+ state, based on the observed line intensities and the angular correlations of the corresponding γ transitions, could not explain the deduced g factor, even under the assumption of a negative g value for the 2_3^+ state.

*Also at CERN, PH Division, CH-1211 Geneva 23, Switzerland, and Department of Physics and Astronomy, Michigan State University, East Lansing, Michigan, USA.

II. EXPERIMENTAL DETAILS

In the present experiment a beam of isotopically pure ^{68}Zn ions was accelerated to an energy of 180 MeV at the Munich Tandem Accelerator, providing intensities of 20 *e*nA on a multilayered target. The latter consisted of 0.44-mg/cm^2 natural carbon deposited on a 3.34-mg/cm^2 Gd layer, which was evaporated on a 1.4-mg/cm^2 Ta foil, backed by a 4.49 mg/cm^2 Cu layer. Between C and Gd, as well as between Ta and Cu, thin layers of natural Ti ($\sim$0.005 mg/cm^2) provided good adherence, which is crucial for the precession experiments. The same target had been used in former measurements under almost identical conditions [7]. The target was cooled to liquid-nitrogen temperature and magnetized to saturation by an external field of 0.06 *T*. The relevant level scheme of ^{68}Zn for Coulomb excitation is shown in Fig. 1 [8]. The excited Zn nuclei move through the Gd layer at mean velocities of $\sim 5.9 v_0$ ($v_0 = e^2/\hbar$), experiencing spin precessions in the transient field, and are ultimately stopped in the hyperfine-interaction-free environment of the Cu backing. The deexcitation γ rays were measured in coincidence with the forward-scattered carbon ions detected in a 100-μm Si detector at 0°. A 5-μm-thick Ta foil between target and particle detector served as a beam stopper that, however, was transparent to the carbon recoils. As in the previous experiments the detector was operated at a very low bias of $\sim$5 V to establish a thin depletion layer for separating the energies of carbon ions from those of light particles as protons and α particles resulting from sub-Coulomb fusion and transfer reactions. Under these conditions very clean γ-coincidence spectra were obtained. Intrinsic Ge detectors of $\sim$40% relative efficiency were used for γ detection. Figure 2 shows a typical coincidence spectrum with emphasis on the ($4_1^+ \rightarrow 2_1^+$) γ line. Evidently all relevant γ lines were well resolved, allowing a rigorous determination of their intensities required for the angular correlations as well as for the precessions of the nuclear states in question.

Particle-γ angular correlations $W(\Theta_\gamma)$ were measured to determine the slope $|S| = [1/W(\Theta_\gamma)][dW(\Theta_\gamma)/d\Theta_\gamma]$ in the rest frame of the γ-emitting nuclei at $\Theta_\gamma^{\text{lab}} = \pm 65^\circ$ and $\pm 115^\circ$, where the sensitivity to the precessions was optimal for all transitions of interest. Precession angles, Φ^{exp}, were derived from counting-rate ratios *R* for "up" and "down" directions of the external magnetizing field, which can be expressed as [7]

$$\Phi^{\text{exp}} = \frac{1}{S}\frac{\sqrt{R}-1}{\sqrt{R}+1} = g\frac{\mu_N}{\hbar}\int_{t_{\text{in}}}^{t_{\text{out}}} B_{\text{TF}}[v_{\text{ion}}(t)]e^{-\frac{t}{\tau}}\,dt, \quad (1)$$

where g is the g factor of the nuclear state and B_{TF} is the transient field acting on the nucleus during the time interval $(t_{\text{out}} - t_{\text{in}})$ that the ions spend in the Gd layer of the target; the exponential accounts for nuclear decay with lifetime τ in the Gd layer. Simultaneously with the precessions, the lifetimes

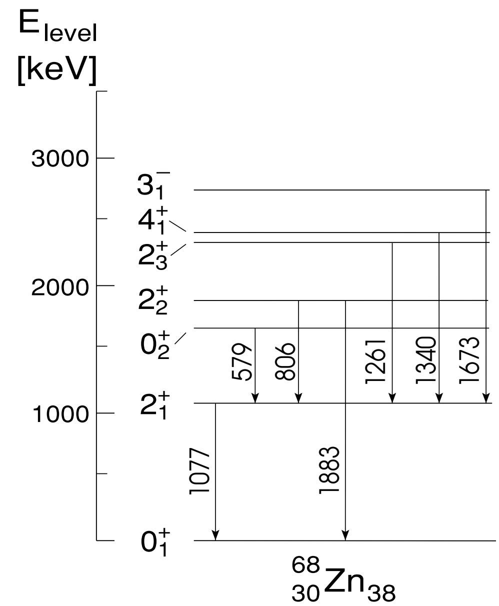

FIG. 1. Level scheme of ^{68}Zn with γ transitions relevant to the present work.

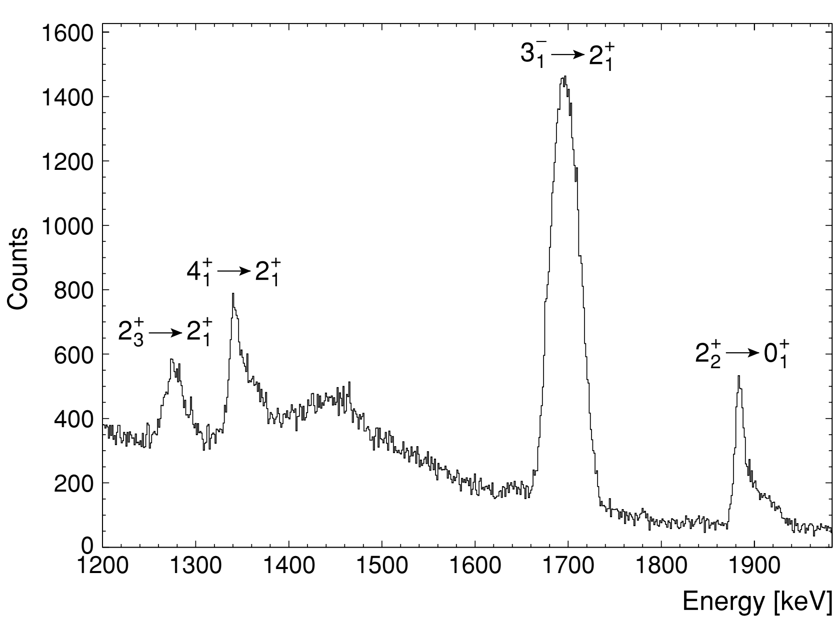

FIG. 2. Relevant γ-coincidence spectrum of a Ge detector placed at $\Theta_\gamma = 65^\circ$ relative to the beam axis. The Doppler-broadened lineshapes reflect the nuclear lifetimes.

TABLE I. Summary of the measured slopes of the angular correlations at $\Theta_\gamma^{\rm lab} = \pm 65^\circ$, precession angles, and lifetimes of excited states in ^{68}Zn. The $\Phi^{\rm lin}/g$ values were calculated with Eqs. (1)–(3). The g factors deduced and the newly determined lifetimes are compared with previous results [6,7].

E_x (MeV)	I^Π	τ (ps)		$\|S(65^\circ)\|$ (mrad)$^{-1}$	$\Phi^{\rm exp}$ (mrad)	$\Phi^{\rm lin}/g$ (mrad)	$g(I)$	
		Present	[7]				Present	[6,7]
1.077	2_1^+	2.34(4)	2.32(5)	2.133(15)	15.2(2)	26.4(26)	+0.58(6)	+0.48(3)
1.883	2_2^+	1.5(1)	1.4(1)	1.24(16)	12(4)	24.9(25)	+0.48(17)	+0.53(15)
2.338	2_3^+	0.47(6)	0.45(4)	—	—	—	—	—
2.417	4_1^+	1.18(8)	1.10(8)	0.85(18)	−6(8)	23.8(24)	−0.3(3)	−0.4(2)
2.751	3_1^-	0.37(1)	0.38(2)	0.310(52)	5(6)	16.7(17)	+0.3(4)	+0.4(3)

of several excited states have been redetermined by use of the Doppler-shift attenuation method. For the analysis of the Doppler-broadened lineshapes, which were observed with a Ge detector placed at 0° to the beam direction, the computer code LINESHAPE [9] has been used. Specific details of the analysis procedure are given in Refs. [6,7].

III. RESULTS AND DISCUSSION

The g factors have been determined from the measured precession angles by calculation of the effective transient field $B_{\rm TF}$ on the basis of the empirical linear parametrization (see Ref. [6,7]):

$$B_{\rm TF}(v_{\rm ion}) = G_{\rm beam} \cdot B_{\rm lin}, \quad (2)$$

with

$$B_{\rm lin} = a({\rm Gd}) \cdot Z_{\rm ion} \cdot v_{\rm ion}/v_0, \quad (3)$$

where the strength parameter $a({\rm Gd}) = 17(1)T$ [7] and $G_{\rm beam} = 0.61(6)$ is the attenuation factor accounting for the demagnetization of the Gd layer induced by the Zn beam (see [7]). The same scheme has been successfully applied in many former measurements.

Precession and lifetime data from a single run are summarized in Table I together with the deduced g factors, which are compared with previous results [6,7]. Evidently all newly determined lifetimes and g factors are in good agreement with earlier data. It is further noted that the average g factor of the 2_1^+ state, $g = +0.48(3)$, which is the average of results of two previous independent measurements, $g = +0.44(5)$ [6], and $g = +0.51(4)$ [7], seems to be slightly smaller than the value obtained in the present experiment. However, all three values are consistent within their individual errors with the quoted mean value, $g = +0.50(3)$ (see Table II). In particular, the g factor of the 4_1^+ state with its negative sign has been confirmed, implying that the previously measured precession is indeed free of any disturbing contributions that were under consideration. The relatively large error in the magnitude of the g factor is of purely statistical origin because of the small excitation cross section of the nuclear state and the low γ-detection efficiency of the Ge detectors. The striking difference in the g factors of the 4_1^+ states between ^{64}Zn and ^{68}Zn is shown in Fig. 3.

In Table II, the g factors and the $B(E2)$'s, both improved in accuracy by averaging with the data of Refs. [6,7], are compared with results from new large-scale shell-model calculations. The need for new calculations is based on the fact that the previous shell-model calculations failed to explain the experimental g factor of the 4_1^+ state in ^{68}Zn. In view of the negative sign of this g factor, it had been suggested that the neutron $0g_{9/2}$ configuration must play a dominant role in the nuclear wave function, which evidently was not accounted for by the former calculations.

To study the importance of the $0g_{9/2}$ orbit we performed shell-model calculations by using ^{56}Ni as the closed shell core, with a model space defined by protons and neutrons occupying the single-particle orbitals $0f_{5/2}$, $1p_{3/2}$, $1p_{1/2}$, and

TABLE II. Comparison of experimental excitation energies, average g factors, and $B(E2)$ values (see also Ref. [7] and refs. therein) of ^{64,68}Zn with results from shell-model (SM) calculations (see text for further details).

Nucleus	$E(I_f^\pi)$ (MeV)			$I_f^\pi \to I_i^\pi$	$\tau(I_f^\pi)$ (ps)	$g(I_f^\pi)$			$B(E2)\downarrow(e^2{\rm fm}^4)$		
	Exp.	SM-1	SM-2			Exp.	SM-1	SM-2	Exp.	SM-1	SM-2
^{64}Zn	0.992		1.057	$2_1^+ \to 0_1^+$	2.77(6)	+0.45(3)		+0.813	307(7)		170.4
	2.307		2.830	$4_1^+ \to 2_1^+$	1.12(4)	+0.53(16)		+1.568	185(7)		196.1
	1.799		2.467	$2_2^+ \to 0_1^+$	2.9(3)	—		+0.334	3.5(4)		1.2
^{68}Zn	1.077	0.765	0.934	$2_1^+ \to 0_1^+$	2.33(3)	+0.50(3)	+0.027	+0.223	242(3)	151.6	190.9
	2.417	1.936	2.097	$4_1^+ \to 2_1^+$	1.14(6)	−0.37(17)	+0.066	+0.008	166(9)	209.2	224.6
	1.883	1.318	1.629	$2_2^+ \to 0_1^+$	1.45(7)	+0.51(11)	+0.672	+0.242	15(1)	26.0	3.4

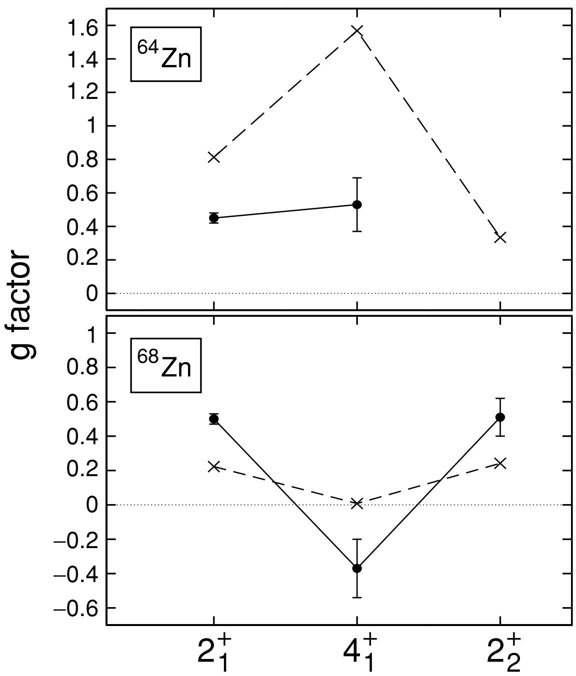

FIG. 3. Comparison of experimental g factors associated with the 2_1^+, 4_1^+, and 2_2^+ states in ^{64}Zn and ^{68}Zn (closed circles) with results from large-scale shell-model calculations (crosses; see text). Lines are drawn to guide the eye.

$0g_{9/2}$ $(0f_{5/2}1p0g_{9/2})$. To determine the effective interaction, we used the recent charge-dependent potential model of Machleidt, the so-called CD-Bonn interaction [10]. We obtained the final effective two-body interaction by means of the many-body perturbation theory to third order, employing a renormalized nucleon-nucleon interaction defined for ^{56}Ni as the closed shell core and including folded diagrams to infinite order. For details, see, for example, Ref. [11]. A harmonic-oscillator basis was used, with an oscillator energy determined by $\hbar\Omega = 45A^{-1/3} - 25A^{-2/3} = 10.1$ MeV, $A = 56$ being the mass number. For the single-particle energies we employed values adapted from Grawe *et al.* in Ref. [12], resulting in the energy differences $\epsilon_{0g_{9/2}} - \epsilon_{1p_{3/2}} = 3.70$ MeV, $\epsilon_{0f_{5/2}} - \epsilon_{1p_{3/2}} = 0.77$ MeV, and $\epsilon_{1p_{1/2}} - \epsilon_{1p_{3/2}} = 1.11$ MeV for neutrons and $\epsilon_{0g_{9/2}} - \epsilon_{1p_{3/2}} = 3.51$ MeV, $\epsilon_{0f_{5/2}} - \epsilon_{1p_{3/2}} = 1.03$ MeV, and $\epsilon_{1p_{1/2}} - \epsilon_{1p_{3/2}} = 1.11$ MeV for protons. The effective interaction was not corrected for any eventual monopole changes. This means that the only parameters that enter our calculations are those defining the nucleon-nucleon interaction fitted to reproduce the scattering data, the experimental single-particle energies, and the oscillator basis. Furthermore, for the computation of the $B(E2)$'s and g factors, we used unrenormalized magnetic moments and the canonical unrenormalized charges for protons and neutrons. The latter entails charges of $1.5e$ and $0.5e$ for protons and neutrons, respectively. The free-nucleon operator for the magnetic moment is defined as

$$\mu_{\rm free} = g_l\mathbf{l} + g_s\mathbf{s}, \tag{4}$$

with $g_l(\text{proton}) = 1.0$, $g_l(\text{neutron}) = 0.0$, $g_s(\text{proton}) = 5.586$, $g_s(\text{neutron}) = -3.826$. Note, however, that the magnetic-moment operator in finite nuclei is modified from the free-nucleon operator because of core-polarization and meson-exchange-current (MEC) corrections [13–15]. The effective operator is defined as

$$\mu_{\rm eff} = g_{l,\rm eff}\mathbf{l} + g_{s,\rm eff}\mathbf{s} + g_{p,\rm eff}[Y_2, \mathbf{s}], \tag{5}$$

where $g_{x,\rm eff} = g_x + \delta g_x$, $x = l, s$, or p, and g_x is the free-nucleon, single-particle g factors ($g_p = 0$) and δg_x the calculated correction to it. Note the presence of a new term $[Y_2, \mathbf{s}]$, absent from the free-nucleon operator, which is a spherical harmonic of rank $\lambda' = 2$ coupled to a spin operator to form a spherical tensor of multipolarity $\lambda = 1$.

In the following calculations we limit ourselves to a calculation with free operators only. The results for the energies of the low-lying excited states for both ^{64}Zn and ^{68}Zn are given in Table II, and $B(E2; 2_1^+ \to 0_1^+)$, $B(E2; 2_2^+ \to 0_1^+)$, and $B(E2; 4_1^+ \to 2_1^+)$ and the g factors $g(2_1^+)$, $g(2_2^+)$, and $g(4_1^+)$ are presented and compared with the available data.

Two types of shell-model results are discussed and shown in this table, SM-1 and SM-2, whereby for ^{64}Zn only SM-2 calculations are performed and for ^{68}Zn both calculations are performed. In SM-1 we limit the number of neutrons that can be excited to the $0g_{9/2}$ orbit to two, whereas SM-2 is the full shell-model calculation. The latter basis is, however, unnecessarily large because the results converge with four neutrons at most in the $0g_{9/2}$ orbit. One sees clearly that with at most two neutrons in the $0g_{9/2}$ orbit, the spectrum of ^{68}Zn is rather poorly reproduced. Even for the fully converged calculation the first excited 0_2^+ state at 1.655 MeV is badly reproduced ($E^{\rm SM-2} = 2.406$ MeV), indicating most likely the need for particle-hole excitations, especially from the $0f_{7/2}$ orbit. The typical occupation probabilities in the SM-2 calculation of the $0g_{9/2}$ neutron single-particle orbit span from 2.2 to 2.4. The $1p_{3/2}$ neutron orbit has an average occupancy of 3.5 particles whereas the low-lying $0f_{5/2}$ neutron orbit has occupancies around three. We note that for the 2_1^+, 2_2^+, and the 4_1^+ excitation energies there is satisfactory agreement with the data.

For ^{68}Zn the calculated $B(E2; 2_1^+ \to 0_1^+)$ exhibits a rather good agreement with the data whereas the $B(E2; 4_1^+ \to 2_1^+)$ is overestimated. This could be ascribed to deficiencies in the two-body Hamiltonian and/or omitted degrees of freedom in the model space. For ^{64}Zn we get 170.4 e^2 fm^4 for the $B(E2; 2_1^+ \to 0_1^+)$, to be compared with the experimental value of 307 e^2fm^4, hinting at the need of larger effective charges. This means in turn that particle-hole excitations involving the $0f_{7/2}$ orbit may be more important for ^{64}Zn than for ^{68}Zn, in agreement with previous shell-model calculations that include this degree of freedom (see Refs. [6,7]).

This behavior is also reflected in the g factors for ^{64}Zn, which tend to be larger than the experimental values. If we, however, introduce effective magnetic moments by assuming a renormalization factor of 0.7 for g_s of protons and neutrons, we obtain g factors closer to experiment. In addition, the $0f_{7/2}$ orbit, if coupled with the $1p_{3/2}$ orbit, can yield a negative contribution to the g factors. The latter analysis is obviously performed at the level of a simple two-body configuration (see, for example, discussions in Refs. [16–18]); however, together with the $(0g_{9/2})^2$ configuration, these are the only two-body configurations of interest here that can yield a *negative g* factor. For ^{64}Zn the occupancy of the $0g_{9/2}$ orbit is less than one and plays therefore a negligible role in the calculation of g factors. Because excitations from the ^{56}Ni closed shell core are also not included in the present model space, this source of reduction for the g factors cannot be accounted for. Thus, for ^{64}Zn, the theoretical values should be larger than the experimental ones, which is indeed the case.

For ^{68}Zn and its g factors we note that for the 2^+ states there is a fair agreement with data, confirming the previous shell-model analysis presented in Refs. [6,7]. For $g(4_1^+)$ we see that there is again a change from the calculation with only two neutrons in the $0g_{9/2}$ orbit to the full calculation. This displays the role played by the $0g_{9/2}$ orbit, which for the 4_1^+ has an average occupation probability of 2.4 in the full SM-2 calculation, much larger than we have for ^{64}Zn. For SM-1 the corresponding occupation probability is 1.99, and this difference is clearly reflected in the change of $g(4_1^+)$ from $+0.066$ to $+0.008$, demonstrating thereby the distinct sensitivity to $(0g_{9/2})^2$ admixtures in the wave function (see also Table II). However, for SM-2 the g factor, although very small, is still positive. Introducing effective magnetic moments reduces the theoretical SM-2 value to $g(4_1^+) = +0.003$. We speculate again whether particle-hole excitations involving the $0f_{7/2}$ orbit could yield further reductions and eventually a negative contribution. Another possibility is to include the effect of MECs, as was done in Ref. [15]. In spite of these omitted degrees of freedom, we see that our model space displays the important role played by the $(0g_{9/2})^2$ neutron configuration when going from the SM-1 to the full SM-2 shell-model calculation, thereby lending support to the experimental analysis.

The important role of the neutron $g_{9/2}$ orbit is also seen in the g factors of the low-lying $9/2^+$ states in odd Zn isotopes with a large negative value ($g \simeq -0.24$ [19]), although smaller in absolute value than the corresponding Schmidt value.

IV. SUMMARY AND CONCLUSIONS

We have remeasured the g factor of the 4_1^+ state in ^{68}Zn with an improved energy resolution of the detectors used. The experimental value, $g(4_1^+) = -0.3(3)$, is consistent with our previous measurement, leading to a weighted mean value of $g(4_1^+) = -0.37(17)$ as the final result. In addition, the accuracy of the g factors of the 2_1^+, 2_2^+, and 3_1^- states has been improved and their lifetimes were well reproduced. The experimental results for ^{64}Zn and ^{68}Zn have been compared with new large-scale shell-model calculations by use of ^{56}Ni as a closed shell core and a model space consisting of protons and neutrons occupying the $0f_{5/2}1p0g_{9/2}$ single-particle orbits. The agreement between theory and experiment is fairly good, and the calculations reproduce well the experimental trends for the g factors from ^{64}Zn to ^{68}Zn, although our theoretical approach is not capable of providing the negative sign of the experimental $g(4_1^+)$ value in ^{68}Zn. This deficiency may be ascribed to particle-hole excitations, with the $0f_{7/2}$ orbit playing a major role. The effect of MECs may also play a role and will be investigated in future works, together with the inclusion of the $0f_{7/2}$ orbit. In view of the present results, similar measurements for the Ge isotones ^{66}Ge and ^{70}Ge are highly desirable to search for corresponding effects in the nuclear wave functions.

ACKNOWLEDGMENTS

Discussions with Alex Brown (MSU) and Georgi Georgiev (CERN) are gratefully acknowledged. The authors are thankful to the operating staff of the Munich tandem accelerator. Support by the Bundesministerium für Bildung, Forschung, und Technologie and the Deutsche Forschungsgemeinschaft is acknowledged. The work of T.E. and M.H.-J. has been supported by the Research Council of Norway (Program for Supercomputing) through a grant of computing time.

[1] R. V. F. Janssens and T. L. Khoo, Annu. Rev. Nucl. Part. Sci. **41**, 321 (1999).
[2] T. Sakuda and S. Ohkubo, Nucl. Phys. **A744**, 77 (2004).
[3] E. Ideguchi *et al.*, Phys. Rev. Lett. **87**, 222501 (2001).
[4] C. E. Svensson *et al.*, Phys. Rev. Lett. **82**, 3400 (1999).
[5] C. E. Svensson *et al.*, Phys. Rev. Lett. **79**, 1233 (1997).
[6] O. Kenn, K. H. Speidel, R. Ernst, S. Schielke, S. Wagner, J. Gerber, P. Maier-Komor, and F. Nowacki, Phys. Rev. C **65**, 034308 (2002).
[7] J. Leske, K.-H. Speidel, S. Schielke, O. Kenn, D. Hohn, J. Gerber, and P. Maier-Komor, Phys. Rev. C **71**, 034303 (2005).
[8] H. Junde and B. Singh, Nucl. Data Sheets **91**, 395 (2000).
[9] J. C. Wells and N. R. Johnson, program LINESHAPE, Oak Ridge National Laboratory (1994) (unpublished).
[10] R. Machleidt, Phys. Rev. C **63**, 024001 (2001).
[11] M. Hjorth-Jensen, T. T. S. Kuo, and E. Osnes, Phys. Rep. **261**, 125 (1995).
[12] H. Grawe, M. Gorska, M. Rejmund, M. Pfützner, M. Lipoglavsek, C. Fahlander, M. Hellström, D. Kast, A. Jungclaus, K. P. Lieb, R. Grzywacz, K. Rykaczewski, B. A. Brown, M. Hjorth-Jensen, and K. H. Maier, in *Highlights of Modern Nuclear Structure*, edited by A. Covello (World Scientific, Singapore, 1999), p. 137.
[13] I. S. Towner, Phys. Rep. **185**, 263 (1987).
[14] B. Castel and I. S. Towner, *Modern Theories of Nuclear Moments* (Clarendon, Oxford, 1990).
[15] B. A. Brown, N. J. Stone, J. R. Stone, I. S. Towner, and M. Hjorth-Jensen, Phys. Rev. C **71**, 044317 (2005).
[16] R. D. Lawson, *Theory of the Nuclear Shell Model* (Clarendon, Oxford, 1980), pp. 295–316.
[17] A. Arima and H. Horie, Prog. Theor. Phys. **11**, 509 (1954).
[18] G. Georgiev, Ph.D. thesis, University of Leuven, Belgium, 2001 (unpublished).
[19] P. Herzog *et al.*, Z. Phys. A **332**, 247 (1989).